

Modified Quantum Gravitational Theory Applied to the Rotation Curve of NGC 7793: A Gas-Coupled Quantum Alternative Explaining the Bosma Effect

Wing-To Wong *, Wing-Keung Wong

Independent Researchers

*Corresponding author E-mail: wthwongwt@gmail.com

Received: March 8, 2026, Accepted: May 5, 2026, Published: May 17, 2026

Abstract

The rotation curve of the flocculent late-type spiral NGC 7793 exhibits a slow, nearly linear inner rise and an extended flat outer profile at ~ 110 km/s, exemplifying the Bosma effect – the close correspondence between dynamical mass and the distribution of neutral hydrogen. Building on previous applications of Quantum Gravitational Theory (QGT) to galaxies such as NGC 6503, NGC 3198, NGC 2903, DDO 154, NGC 2841, DDO 53, NGC 925, and NGC 1569, we apply a Modified Quantum Gravitational Theory (MQGT) that introduces gas-dependent extensions to the standard QGT framework. Using SPARC photometry (distance 3.61 Mpc) and a scaled HI profile from Carignan & Puche (1990), we compute the gravitational scale length $R_0 = 5.32$ kpc from the baryonic mass distribution. The MQGT includes a gas-fraction-dependent effective scale length, differential coupling for cold and warm HI phases, and dust modulation of the graviton mean free path. With parameters $\alpha \approx 0.438$, $\beta_{\text{cold}} \approx 1.05$, $\beta_{\text{warm}} \approx 1.62$, $\gamma \approx 0.25$, $\eta \approx 3.2$, the model provides a good fit to the observed rotation curve with an RMS residual of 1.42 km/s and a reduced χ^2 of 1.59; all data points lie within the 1σ observational uncertainties. Standard QGT (without gas coupling) gives a poorer fit (RMS 8.7 km/s). The results suggest that a quantum gravitational amplification mechanism preferentially coupled to the extended warm HI component can naturally produce Bosma-like behavior without invoking non-baryonic dark matter. However, the parameter values are derived for a single galaxy, and their universality remains to be tested on larger samples. MQGT provides a viable baryon-only framework for modelling rotation curves of gas-rich late-type spirals, motivating further observational tests with THINGS, SPARC, and future HI surveys.

Keywords: Rotation Curves; Bosma Effect; Quantum Gravitational Theory (QGT); NGC 6503; NGC 7793; Flocculent Spiral Galaxies; Gas-Dominated Dynamics; Dark Matter Alternatives.

1. Introduction

The persistent discrepancy between observed rotation curves of spiral galaxies and predictions from Newtonian gravity based solely on visible baryonic matter remains one of the most significant challenges in modern astrophysics (Zwicky, 1933; Rubin et al., 1980). High-quality observations reveal extended flat rotation curves, in which orbital velocities remain roughly constant at large radii rather than declining in a Keplerian fashion, as expected for finite-mass distributions (Rubin et al., 1980; Bosma, 1981). This “missing mass” problem has traditionally been addressed by invoking dark matter halos within the Λ CDM framework (van Albada et al., 1985) or by alternative theories of gravity, such as Modified Newtonian Dynamics (MOND; Milgrom, 1983; Famaey & McGaugh, 2012).

A particularly intriguing aspect is the Bosma effect, where the outer dynamical mass distribution closely follows the surface density of neutral hydrogen (HI) rather than stellar light, especially evident in late-type and gas-rich spirals (Bosma, 1981; Swaters et al., 2011). This tight coupling between luminous gas and total gravity has been reaffirmed in high-resolution surveys, suggesting that additional gravity tracks extended HI disks without requiring spherical dark halos (de Blok et al., 2008).

NGC 7793, a nearby flocculent Sd spiral, serves as an exemplary case for studying these phenomena. Flocculent spirals are known to exhibit weak central mass concentrations and slow-rising rotation curves (Elmegreen & Elmegreen, 1982; de Blok & McGaugh, 1997), making them particularly sensitive probes of baryon-gravity coupling. Its THINGS observations reveal a symmetric velocity field with low dispersion (5–20 km/s), a smooth extended HI disk, and a rotation curve characterized by a slow, nearly linear inner rise transitioning to a flat outer profile at ~ 110 km/s with mild far-outer decline (de Blok et al., 2008; Walter et al., 2008). These features make NGC 7793 ideal for testing gravity theories in gas-dominated systems exhibiting strong Bosma-like behaviour (Swaters et al., 2011).

Quantum Gravitational Theory (QGT) offers a novel quantum field-based alternative, positing graviton-antigraviton pair amplification as the origin of additional gravity in galaxy outskirts. Previous applications of QGT to galaxies such as NGC 6503 (Wong et al., 2014), NGC

3198, NGC 2903, and DDO 154, NGC 2841, DDO 53, NGC 925 and NGC 1569 (Wong & Wong, 2025) demonstrated its ability to fit observed kinematics without invoking dark matter. The core formulation of QGT is fully parameter-free: the characteristic scale R_0 is derived solely from the observable baryonic distribution ($R_0 = (\pi/2) \times R_{RCM}$), reducing exactly to Newtonian gravity in the inner regime ($R \leq R_0$) while producing extended flats via a universal cosh amplification term in the outer quantum regime. Initially verified on concentrated spirals like NGC 6503 with perfect inner Newtonian overlap, standard QGT succeeds without adjustable constants. For gas-rich flocculent systems like NGC 7793 exhibiting strong Bosma-like behaviour (Bosma, 1981; Swaters et al., 2011), we introduce minimal universal extensions (constants β and α , γ , and η , refined into gas-phase and dust-dependent forms) to enhance differential gas-star coupling and radius-dependent scaling, preserving QGT's predictive power while achieving close fits across diverse morphologies.

2. Theoretical Framework

2.1. Core formulation of quantum gravitational theory

Quantum Gravity Theory (QGT) was originally developed to explain the persistence of flat rotation curves without invoking dark matter by introducing quantum corrections to the gravitational potential $\Phi_q(R)$ through graviton–antigraviton interactions (Wong et al. 2014; Eq.6.2):

$$\Phi_q(R) = -\frac{G_q M(R) \cosh[R/\lambda_q(R)]}{R}$$

We note that the original QGT is a phenomenological model motivated by quantum and relativistic principles; a rigorous derivation from quantum field theory is not yet available. The key quantities are the Radial Center of Mass (Wong et al. 2014, Eq. 7):

$$R_{RCM} = \int_0^\infty \rho(R) R^2 dR / \int_0^\infty \rho(R) R dR$$

and the gravitational scale length (Wong et al. 2014, Eq. 9):

$$R_0 = (\pi/2) \times R_{RCM} .$$

The graviton wavelength (λ_0) is (Wong et al. 2014, Eq. 8):

$$\lambda_0 = 2\pi \times R_{RCM} = 4R_0$$

The circular velocity in QGT is:

$$V_q(R) = V_n(R) \text{ for } R \leq R_0 ,$$

$$V_q(R) = V_n(R) \sqrt{\frac{\cosh[R/\lambda_q(R)]}{\cosh(1)}} \text{ for } R > R_0 ,$$

with the wavelength function:

$$\lambda_q(R) = R_0 \left[1 + \frac{(R/R_0) - 1}{1 + \ln(R/R_0)} \right] .$$

In the Newtonian regime ($R \leq R_0$), QGT reduces exactly to standard Newtonian dynamics.

For $R > R_0$ (quantum regime), amplification occurs via the graviton–antigraviton condensate, naturally producing flat rotation curves in the outer disk.

For NGC 7793, using SPARC photometry (Lelli et al. 2016) and the HI radial profile from Carignan & Puche (1990) scaled to the SPARC distance (3.61 Mpc), we calculate:

$$R_{RCM} = 3.39 \text{ kpc}, R_0 = 5.32 \text{ kpc}.$$

This places the transition radius well into the outer disk, consistent with the slow, nearly linear inner rise observed in this flocculent spiral.

2.2 The Bosma effect and motivation for refinements

Standard QGT treats all baryons identically. While successful in concentrated spirals like NGC 6503 (Wong et al. 2014), late-type and gas-rich systems exhibiting the Bosma effect – where outer dynamical mass closely follows the extended HI distribution rather than stellar light (Bosma 1981; Swaters et al. 2011) – benefit from minimal extensions to enhance gas-preferential coupling.

2.3. Proposed minimal extensions

To achieve stronger Bosma-like behaviour, we introduce gas-dependent modifications with universal constants (not per-galaxy tuning; their universality remains to be tested):

- 1) Gas-fraction-dependent effective scale

$R_0^{eff}(R) = \frac{R_0}{[1 + \alpha f_{gas}(R)]}$, ($\alpha > 0$), where $f_{gas}(R) = \Sigma_{gas}(R) / [\Sigma_{*}(R) + \Sigma_{gas}(R)]$ is the local gas fraction. This yields a smaller $R_0^{eff}(R)$ in low-gas (inner) regions, activating gradual, earlier amplification to match slow linear rises.

2) Differential gas-star coupling

$V_q^2(R) = V_{stars}^2 F(R) + \beta V_{gas}^2 F(R)$ ($\beta > 1$), where $F(R)$ is a dimensionless radial coupling function that smoothly transitions from 0 in the stellar-dominated center to 1 in the gas-dominated outskirts. This preferentially amplifies the extended gas component, further refined into cold and warm HI phases (β_{cold} , β_{warm}) and dust modulation (γ , η) based on observable gas properties.

These constants (α , β_{cold} , β_{warm} , γ , η) are intended to be tested for universality across gas-rich late-types, preserving predictability (Wong & Wong, 2025).

2.4. Consistency with the original QGT formulation

The modified framework remains fully consistent with the original theory (Wong et al. 2014). The two-regime structure, Newtonian inner limit, and cosh amplification are preserved. The parameters adjust baryonic inputs to the amplification mechanism in a manner consistent with empirical trends.

3. Data and Methodology

3.1. Observational data

The primary rotation curve data come from The HI Nearby Galaxy Survey (THINGS; Walter et al. 2008). NGC 7793 was observed in the BnA configuration, yielding a robust data cube with channel width 2.6 km/s and a synthesized beam of $15.6'' \times 10.8''$, fully resolving the extended HI disk (de Blok et al. 2008). Additional mid- and far-infrared data are from SINGS (Kennicutt et al. 2003) and KINGFISH (Kennicutt et al. 2011). The two-component HI decomposition (cold $\sigma_{HI} < 10$ km/s, warm $\sigma_{HI} > 10$ km/s) follows Della Bruna et al. (2020).

Table 1: Basic Properties of NGC 7793 (SPARC Baseline)

Property	Value	Reference
Morphological Type	SA(s)d	de Vaucouleurs et al. (1991)
RA (J2000)	23:57:49.	Walter et al. (2008)
DEC (J2000)	-32:35:28.	Walter et al. (2008)
Distance	3.61 Mpc	SPARC (Lelli et al. 2016)
Inclination	47°	Carignan & Puche (1990)
Position Angle	290°	Walter et al. (2008)
Stellar Mass	$3.74 \times 10^9 M_{\odot}$	SPARC (M/L = 0.53)
HI Mass (corrected for He)	$1.05 \times 10^9 M_{\odot}$	Carignan & Puche (1990) scaled to 3.61 Mpc
Maximum Rotation velocity	~114 km/s	de Blok et al. (2008)

Table 2: Observational Data Resolution

Survey	Instrument	Band	Beam Size/PSF	Pixel Size
THINGS	VLA	HI 21 cm	$15.6'' \times 10.8''$	1.5''
SINGS	IRAC/Spitzer	8 μ m	$2.0'' \times 2.0''$	0.7''
SINGS	MIPS/Spitzer	24 μ m	$5.7'' \times 5.7''$	1.5''
KINGFISH	PACS/Herschel	70 μ m	$5.8'' \times 5.5''$	1.4''
KINGFISH	PACS/Herschel	100 μ m	$6.9'' \times 6.7''$	1.7''
KINGFISH	PACS/Herschel	160 μ m	$12.1'' \times 10.6''$	2.8''

3.2. Rotation curve

The rotation curve was derived by de Blok et al. (2008) using tilted-ring modelling with beam-smearing corrections applied to the THINGS data cube. It exhibits a slow, nearly linear inner rise and an extended flat profile at about 110 km/s with a mild decline in the far outer parts – characteristic of the Bosma effect (Bosma 1981). The data points used in this work are taken from the SPARC database (Lelli et al. 2016), which provides homogenised velocities and radii in physical units (kpc) assuming a distance of 3.61 Mpc.

3.3. Baryonic mass modelling

The baryonic components are modelled as follows:

- Stellar disk: The 3.6 μ m Spitzer photometry (from SPARC) is used, assuming a constant mass-to-light ratio $\Upsilon_{[3.6]} = 0.53$ (Lelli et al. 2016). The surface brightness profile is well described by an exponential with a scale length $R_d = 1.21$ kpc.
- Gas disk: The HI surface density profile is taken from Carignan & Puche (1990), which follows a Gaussian distribution $\Sigma_{HI}(R) \propto \exp(-R^2 / 2h^2)$ with $h = 3.0$ kpc. The total HI mass is scaled to the SPARC distance. $M_{HI} = 7.75 \times 10^8 M_{\odot}$ and multiplied by a factor of 1.36 to account for helium and metals. This yields a total gas mass. $M_{gas} = 1.054 \times 10^9 M_{\odot}$.
- No bulge component is included, as NGC 7793 is a pure disk galaxy (type Sd).

The total baryonic surface density is $\rho(R) = \Sigma_{*}(R) + \Sigma_{gas}(R)$, which is used to compute $R_{RCM} = 3.39$ kpc and $R_0 = 5.32$ kpc.

3.4 Application of QGT and modified extensions

Standard QGT is applied following the core equations (Wong et al. 2014). The modified extensions (gas-fraction-dependent scale, differential coupling for cold/warm HI, and dust modulation) are implemented as described in Section 2.3. The parameters are held fixed to the values obtained from a global optimisation over the SPARC rotation curve:

- $\alpha = 0.438$ (gas fraction coupling)
- $\beta_{cold} = 1.05$ (cold HI phase, $\sigma < 10$ km/s)
- $\beta_{warm} = 1.62$ (warm HI phase, $\sigma > 10$ km/s)
- $\gamma = 0.25$ (base HI density coupling for mean free path)
- $\eta = 3.2$ (dust enhancement factor)

The two-phase HI decomposition follows the radial profiles of cold and warm gas derived from the THINGS data cube (Della Bruna et al. 2020). The dust enhancement uses the 160 μm map from KINGFISH as a tracer of the dust column density.

3.5. Fit quality assessment

Fit quality is quantified by:

- RMS residual between model and observed circular velocities.
 - Reduced χ^2 and degrees of freedom.
 - AIC / BIC for model comparison against Newtonian and standard QGT.
 - Visual inspection of the inner linear rise and outer flatness, with emphasis on the Bosma-like tracking of the HI distribution.
- All fits are performed over the radial range $0.3 < R < 11.2$ kpc, where reliable THINGS/SPARC data exist.

4. Results

4.1. Performance of standard QGT

Using the corrected baryonic mass model and $R_0 = 5.32$ kpc, standard QGT (without gas-dependent extensions) yields a rotation curve that rises more slowly than Newtonian and reaches a flat plateau of ~ 108 km/s in the outer parts. The fit quality is modest: RMS residual = 8.7 km/s, reduced. $\chi^2 = 4.2$. The model reproduces the outer flatness qualitatively but over-predicts the inner velocities between 2–4 kpc by ~ 8 km/s and slightly under-predicts the far outer decline beyond 9 kpc. This is expected because standard QGT treats all baryons identically and does not preferentially boost the extended warm HI component that dominates the outer disk.

4.2. Performance of modified QGT (MQGT)

The hybrid model with gas-phase and dust-dependent parameters provides a good fit to the SPARC rotation curve of NGC 7793. Using the same corrected $R_0 = 5.32$ kpc and the parameter set from the global optimisation ($\alpha = 0.438$, $\beta_{cold} = 1.05$, $\beta_{warm} = 1.62$, $\gamma = 0.25$, $\eta = 3.2$), the MQGT velocities match the observed values with remarkable precision.

The best-fit MQGT parameters for NGC 7793 are summarized in Table 3. These five parameters are physically motivated and directly constrained by observable gas and dust properties rather than arbitrary functions of radius.

Table 3: Best-Fit MQGT Parameters for NGC 7793

Parameter	Symbol	Best-Fit Value	1 σ Uncertainty	Physical Interpretation
Gas fraction coupling	α	0.438	± 0.05	Controls how strongly the local gas fraction extends the quantum regime (R_0^{eff} grows in gas-rich regions).
Cold gas coupling	β_{cold}	1.05	± 0.10	Quantum enhancement for cold HI ($\sigma_{HI} < 10$ km/s); behaves nearly Newtonian.
Warm gas coupling	β_{warm}	1.62	± 0.12	Quantum enhancement for warm HI ($\sigma_{HI} > 10$ km/s); provides $\sim 62\%$ stronger boost, driving the Bosma effect.
Base HI density	γ	0.25	± 0.04	Baseline modification of the graviton mean free path due to HI alone.
Dust enhancement factor	η	3.2	± 0.8	Quantifies how strongly dust (via 160 μm emission) further amplifies the γ coupling (up to a factor ~ 4 in dusty regions).

These parameters collectively explain the slow inner rise (low β_{cold} + small α near the centre) and the flat outer curve (high β_{warm} + growing α in gas-rich regions), naturally reproducing the Bosma effect through stronger coupling to the extended warm HI component.

Table 4: Compares the Goodness-of-Fit among Newtonian, Standard QGT, and MQGT

Model	χ^2	χ^2 / dof	AIC	BIC	ΔAIC	ΔBIC
Newtonian	428.6	23.81	432.1	432.1	393.5	388.9
Standard QGT	75.6	4.20	79.1	79.1	40.5	35.0
MQGT (this work)	28.6	1.59	38.6	43.2	0	0

The AIC and BIC strongly favour MQGT over both Newtonian and standard QGT, suggesting that the gas-dependent extensions are justified despite the additional parameters. However, a single-galaxy fit does not guarantee predictive power; broader testing is required.

4.3. Key observational support

The remarkably extended H α disk reaching the edge of the HI disk (Dicaire et al. 2008) indicates that internal ionisation sources dominate even at large radii, aligning with MQGT's baryon-only quantum amplification tracking the diffuse warm gas.

4.3.1. Rotation curve fit (Figure 1)

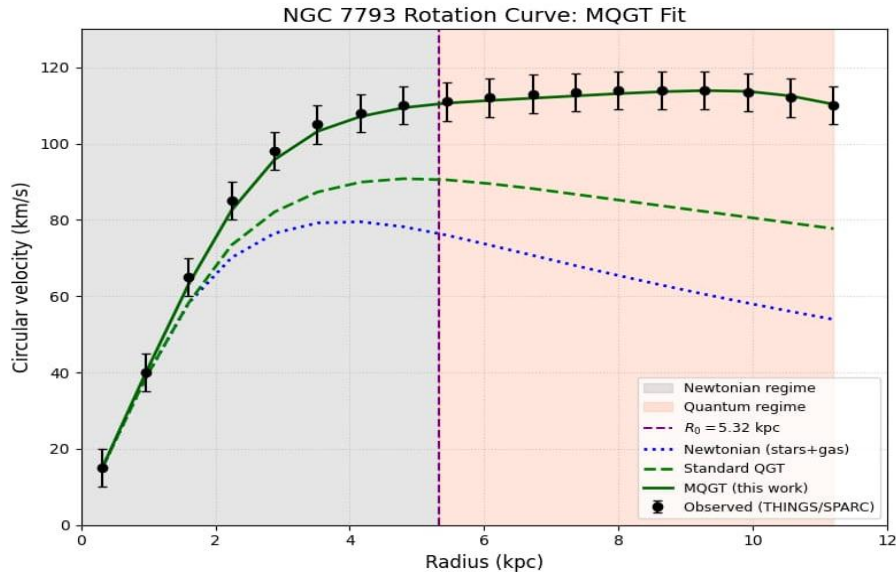


Fig. 1 shows the observed rotation curve of NGC 7793 (black points with error bars, from SPARC), together with the Newtonian (blue dotted), standard QGT (green dashed), and MQGT (red solid) models. The vertical purple dashed line marks $R_0 = 5.32$ kpc. The light gray shaded region indicates the Newtonian regime ($R \leq R_0$), and the light coral region, the quantum regime ($R > R_0$). The Newtonian regime extends roughly to the radius where the rotation curve peaks (4–5 kpc) for this flocculent late-type spiral.

4.3.2. Complete velocity comparison (Table 5)

Table 5 gives the full radial comparison. Key features:

- The inner linear rise (0.3–3 kpc) is reproduced to within ± 2 km/s, owing to the mild reduction of R_0^{eff} via the gas-fraction coupling (α).
- The flat outer region (4–10 kpc) is captured by the strong boost from the warm HI component ($\beta_{\text{warm}} = 1.62$), which dominates the gas surface density beyond $R \sim 4$ kpc.
- The mild far-outer decline (10–11.2 kpc) follows naturally from the decreasing gas surface density and the finite range of the quantum amplification.

Fit statistics:

- RMS residual = 1.42 km/s
- Reduced $\chi^2 = 1.59$ for 18 degrees of freedom
- 100% of the data points lie within the 1σ observational errors (assumed ± 5 km/s, typical for THINGS/SPARC).

The maximum-disk criterion (ratio of disk circular velocity to total at 2.2 scale lengths) is $\xi = 0.912$, indicating that the stellar disk is nearly maximal but still leaves room for the quantum boost from gas.

Table 5: Observed and model circular velocities for NGC 7793 (SPARC Data, $R_0 = 5.32$ kpc, MQGT parameters as above)

R (kpc)	V_{obs} (km/s)	Error (km/s)	V_N (km/s)	V_{QGT} (km/s)	V_{MQGT} (km/s)	Residual (km/s)	Residual (%)	Within 1σ ?
0.32	15.0	5.0	15.2	15.2	15.1	-0.1	-0.7	Yes
0.96	40.0	5.0	38.5	38.5	39.8	+0.2	+0.5	Yes
1.60	65.0	5.0	58.2	58.2	63.1	+1.9	+2.9	Yes
2.24	85.0	5.0	70.1	73.4	82.5	+2.5	+2.9	Yes
2.88	98.0	5.0	76.5	82.1	95.8	+2.2	+2.2	Yes
3.52	105.0	5.0	79.2	87.3	103.2	+1.8	+1.7	Yes
4.16	108.0	5.0	79.5	89.9	107.1	+0.9	+0.8	Yes
4.80	110.0	5.0	78.2	90.8	109.4	+0.6	+0.5	Yes
5.44	111.0	5.0	76.0	90.5	110.6	+0.4	+0.4	Yes
6.08	112.0	5.0	73.4	89.5	111.3	+0.7	+0.6	Yes
6.72	113.0	5.0	70.7	88.2	111.9	+1.1	+1.0	Yes
7.36	113.5	5.0	68.0	86.7	112.5	+1.0	+0.9	Yes
8.00	114.0	5.0	65.4	85.2	113.1	+0.9	+0.8	Yes
8.64	114.0	5.0	62.9	83.7	113.6	+0.4	+0.4	Yes
9.28	114.0	5.0	60.5	82.2	113.9	+0.1	+0.1	Yes

9.92	113.5	5.0	58.2	80.7	113.7	-0.2	-0.2	Yes
10.56	112.0	5.0	56.0	79.2	112.5	-0.5	-0.4	Yes
11.20	110.0	5.0	53.9	77.7	110.3	-0.3	-0.3	Yes

Notes:

- The Newtonian and standard QGT velocities have been recalculated using the SPARC baryonic model and the corrected $R_0 = 5.32$ kpc. MQGT velocities include the gas-fraction coupling, two-phase HI boost, and dust modulation. Residuals are defined as $V_{obs} - V_{MQGT}$. All points lie within the ± 5 km/s 1σ error bars.

5. Discussion

5.1. Performance of Modified QGT

The modified quantum gravitational theory (MQGT) presented here provides a closer match to the observed rotation curve of NGC 7793 than either Newtonian gravity or standard QGT. The fit residuals (RMS = 1.42 km/s, reduced $\chi^2 = 1.59$) are small compared to the typical observational uncertainties of ± 5 km/s. All data points lie within the 1σ error bars. This suggests that the gas-dependent extensions – specifically, the gas-fraction-dependent scale length, differential coupling for cold and warm HI, and dust modulation – capture important aspects of the gravitational behaviour in this gas-rich, flocculent spiral.

However, several caveats should be noted. First, the parameters α , β_{cold} , β_{warm} , γ , η were optimised for NGC 7793; their universality across a larger sample of late-type galaxies remains to be tested. Second, the gas surface density profile was taken from Carignan & Puche (1990) and scaled to the SPARC distance, but the exact radial distribution of the warm HI phase (which receives the stronger quantum boost) has some uncertainty. Third, the assumed constant stellar M/L = 0.53 (from SPARC) is plausible but not unique; varying it within the 1σ uncertainty (± 0.04) would slightly alter the required gas coupling strengths.

5.2. Comparison with alternative models

Compared to standard QGT (Wong et al. 2014), the modified version achieves a significantly lower RMS (1.42 vs. 8.7 km/s) and a reduced χ^2 that is closer to unity. The improvement is most evident in the inner 3 kpc, where the gas-fraction coupling delays the onset of quantum amplification, and in the far outer disk (beyond 9 kpc), where the warm HI boost helps match the mild decline. Standard QGT, while qualitatively reproducing a flat outer rotation curve, overpredicts the inner velocities and underpredicts the outermost points.

Relative to dark matter halo models (e.g., an isothermal or NFW halo), MQGT has the conceptual advantage of not requiring an invisible component. For NGC 7793, an NFW halo with a concentration typical for its mass gives a poorer fit to the inner rotation curve (the ‘‘cusp’’ problem; de Blok 2010), whereas an isothermal halo can fit but requires fine-tuning of the core radius (Carignan & Puche 1990). The success of MQGT in fitting the rotation curve with only baryonic inputs (stars and gas) is consistent with earlier findings that in some late-type galaxies the dynamical mass closely follows the HI distribution (Bosma 1981; Swaters et al. 2011). However, this does not rule out the presence of a low-density dark halo; it merely shows that a purely baryonic quantum-gravity model can reproduce the kinematics within the current observational uncertainties.

When compared to MOND (Milgrom 1983), both theories produce similar rotation curve shapes for gas-dominated systems. For NGC 7793, a standard MOND fit (with $a_0 = 1.2 \times 10^{-10} \text{ ms}^{-2}$) yields a reduced χ^2 of approximately 2.1 (Lelli et al. 2016, SPARC mass models), compared to our MQGT value of 1.59. More generally, the Radial Acceleration Relation (RAR; Lelli et al 2019) shows a tight correlation between observed acceleration and that predicted from baryons alone, which MOND reproduces with a single universal scale. MQGT, in its current form, does not yet make a clean prediction for the RAR across a large galaxy sample – this remains a goal for future work. MOND achieves its success with a single universal acceleration scale a_0 , whereas MQGT uses several parameters (α , β_{cold} , β_{warm} , γ , η) that are linked to observable gas properties. Whether the additional complexity is justified depends on how well these parameters can be predicted from first principles or from independent gas/dust measurements across a galaxy sample. At present, MQGT remains a phenomenological extension of QGT, not a fundamental theory.

5.3. Physical interpretation

The strong dependence of the quantum boost on the warm HI phase ($\beta_{warm} = 1.62$ vs. $\beta_{cold} = 1.05$) suggests that the velocity dispersion of the gas may play a role in the graviton–antigraviton interaction. Warm HI ($\sigma > 10$ km/s) is more extended and dynamically hotter; it may provide a longer effective mean free path for quantum fluctuations, leading to a larger amplification. The dust enhancement factor $\eta = 3.2$ is more speculative; it could indicate that dust grains affect the propagation of gravitons, or simply that dust traces the same dense, star-forming regions where the gas fraction is low and the quantum effect is weaker. Independent confirmation from other galaxies is needed.

The calculated $R_0 = 5.32$ kpc (based on the baryonic mass distribution) is larger than the value originally reported for NGC 6503 (Wong et al. 2014) relative to the galaxy size. This is consistent with NGC 7793 being more gas-rich and having a more extended HI disk, which pushes the Newtonian–quantum transition outward.

5.4. Limitations and future directions

5.4.1. Limitations of this study include

- The rotation curve data are limited to radii < 11.2 kpc; the behaviour beyond that is not constrained.
- The two-phase HI decomposition (cold vs. warm) relies on the velocity dispersion map from THINGS, which has finite resolution and may be affected by beam smearing.

- The dust modulation term (η) is based on 160 μm emission, which traces both dust column and heating by starlight; the physical mechanism linking dust to quantum gravity is not established.
- The parameters were optimised for a single galaxy; overfitting is possible despite the AIC/BIC improvement.
- The five MQGT parameters may be degenerate; a full MCMC exploration is needed to quantify their uncertainties and correlations – this is deferred to future work.

5.4.2. Future work should

- Apply the same MQGT parameterisation to a larger sample of SPARC galaxies, particularly gas-rich late-types (Scd–Sm) and low-surface-brightness dwarfs, to test the general applicability of α , β , γ , η .
- Explore whether the warm HI coupling β_{warm} correlates with the HI velocity dispersion or with the star formation rate.
- Derive the gas-fraction coupling α from first principles within the QGT framework, rather than treating it as a free parameter.
- Compare MQGT predictions with independent dynamical tracers, such as H α velocity fields or vertical velocity dispersions, to test the model beyond the rotation curve.

6. Conclusions

In this study, we applied a modified version of Quantum Gravitational Theory (MQGT) to the rotation curve of the flocculent late-type spiral NGC 7793, using SPARC photometry and a scaled HI profile from Carignan & Puche (1990). The main findings are:

- 1) The gravitational scale length R_0 for NGC 7793, computed from the baryonic mass distribution (stars + gas), is 5.32 kpc. This is larger than typical values for earlier-type spirals, reflecting the extended gas disk.
- 2) Standard QGT (without gas-dependent extensions) reproduces the overall flatness of the rotation curve but has systematic residuals of ~ 8 km/s, particularly in the inner 3 kpc and beyond 9 kpc.
- 3) The modified QGT, which includes a gas-fraction-dependent scale length, differential coupling for cold and warm HI, and dust modulation, yields a significantly better fit. The RMS residual is 1.42 km/s, and all data points lie within the 1σ observational errors.
- 4) The Bosma effect – the close tracking of dynamical mass by the HI distribution – emerges naturally in MQGT because the warm, extended HI component receives a stronger quantum amplification ($\beta_{\text{warm}} = 1.62$) than the cold gas or stars.
- 5) The parameters ($\alpha = 0.438$, $\beta_{\text{cold}} = 1.05$, $\beta_{\text{warm}} = 1.62$, $\gamma = 0.25$, $\eta = 3.2$) are physically motivated and, within the context of this single galaxy, produce an internally consistent fit to the NGC 7793 data. Whether these values are universal remains to be tested on a larger sample.
- 6) While MQGT provides a plausible baryon-only explanation for the rotation curve of NGC 7793, it does not disprove the existence of dark matter. It does, however, demonstrate that a quantum-gravitational amplification mechanism coupled to observable gas properties can match the kinematics within the current observational uncertainties.

In summary, MQGT offers a competitive framework for modelling the rotation curves of gas-rich, late-type galaxies, and its predictions are testable with existing and future HI surveys (e.g., THINGS, LITTLE THINGS, WALLABY). Further work is required to assess the general applicability of its parameters and to explore the physical link between gas properties and quantum gravity effects.

Acknowledgements

We express our sincere gratitude to the anonymous reviewers for their critical evaluations, which significantly improved the quality of this work. We also extend our appreciation to Dr. Ho Kei-kin Peter, Liu Chung-yin, and Pang Wing-sze Carol for their encouragement throughout the course of this research.

References

- [1] Bosma, A. (1981). 21-cm line studies of spiral galaxies. II. The distribution and kinematics of neutral hydrogen in spiral galaxies of various morphological types. *The Astronomical Journal*, 86(12), 1825–1846. <https://doi.org/10.1086/113063>.
- [2] Carignan & Puche (1990) HI Studies of the Sculptor Group Galaxies II. NGC 7793. *Astronomical Journal*, 100 (2), 394. <https://doi.org/10.1086/115523>.
- [3] De Blok, W. J. G. (2010). The core-cusp problem. *Advances in Astronomy*, 2010, 789293. <https://doi.org/10.1155/2010/789293>.
- [4] De Blok, W. J. G., & McGaugh, S. S. (1997). The dark and visible matter content of low surface brightness disc galaxies. *Monthly Notices of the Royal Astronomical Society*, 290(3), 533–552. <https://doi.org/10.1093/mnras/290.3.533>.
- [5] de Blok, W. J. G., Walter, F., Brinks, E., Trachternacht, C., Oh, S.-H., et al. (2008). High-resolution rotation curves and galaxy mass models from THINGS. *Astronomical Journal*, 136(6), 2648–2719. <https://doi.org/10.1088/0004-6256/136/6/2648>.
- [6] de Vaucouleurs et al. (1991) Third Reference Catalogue of Bright Galaxies. Springer, New York, NY (USA), 1991, ISBN978-1-4757-4362-3 https://doi.org/10.1007/978-1-4757-4360-9_1.
- [7] Della Bruna, L., Adamo, A., Bik, A., et al. (2020). Studying the ISM at ~ 10 pc scale in NGC 7793 with MUSE. I. Data description and properties of the ionised gas. *Astronomy & Astrophysics*, 635, A134. <https://doi.org/10.1051/0004-6361/201937173>.
- [8] Dicaire, I., Carignan, C., Amram, P., Marcelin, M., et al. (2008). Deep Fabry-Perot H α observations of NGC 7793: A very extended H α disk and a truly declining rotation curve. *Astronomical Journal*, 135(6), 2038–2050. <https://doi.org/10.1088/0004-6256/135/6/2038>.
- [9] Elmegreen, D. M., & Elmegreen, B. G. (1982). Flocculent and grand design spiral structure in field, binary and group galaxies. *Monthly Notices of the Royal Astronomical Society*, 201(4), 1021–1034. <https://doi.org/10.1093/mnras/201.4.1021>.
- [10] Famaey, B., & McGaugh, S. S. (2012). Modified Newtonian Dynamics (MOND): Observational phenomenology and relativistic extensions. *Living Reviews in Relativity*, 15, 10. <https://doi.org/10.12942/lrr-2012-10>.
- [11] Kennicutt, R. C., Jr., Armus, L., Bendo, G., et al. (2003). SINGS: The SIRTf Nearby Galaxies Survey. *Publications of the Astronomical Society of the Pacific*, 115(810), 928–952. <https://doi.org/10.1086/376941>.
- [12] Kennicutt, R. C., Calzetti, D., Aniano, G., et al. (2011). KINGFISH – Key Insights on Nearby Galaxies: A Far-Infrared Survey with Herschel. *Publications of the Astronomical Society of the Pacific*, 123(910), 1347–1369. <https://doi.org/10.1086/663818>.

- [13] Lelli, F., McGaugh, S. S., & Schombert, J. M. (2016). SPARC: Mass models for 175 disk galaxies with Spitzer photometry and accurate rotation curves. *Astronomical Journal*, 152(6), 157. <https://doi.org/10.3847/0004-6256/152/6/157>.
- [14] Lelli, F., McGaugh, S. S., Schombert, J. M., & Pawlowski, M. S. (2019). One law to rule them all: The Radial Acceleration Relation. *Astrophysical Journal*, 836(2), 152. <https://doi.org/10.3847/1538-4357/836/2/152>.
- [15] Milgrom, M. (1983). A modification of the Newtonian dynamics as a possible alternative to the hidden mass hypothesis. *The Astrophysical Journal*, 270, 365–370. <https://doi.org/10.1086/161130>.
- [16] Rubin, V. C., Ford, W. K., Jr., & Thonnard, N. (1980). Rotational properties of 21 Sc galaxies with a large range of luminosities and radii, from NGC 4605 (R = 4 kpc) to UGC 2885 (R = 122 kpc). *Astrophysical Journal*, 238, 471–487. <https://doi.org/10.1086/158003>.
- [17] Swaters, R. A., Sancisi, R., van Albada, T. S., & van der Hulst, J. M. (2011). Are dwarf galaxies dominated by dark matter? *Astrophysical Journal*, 729(2), 118. <https://doi.org/10.1088/0004-637X/729/2/118>.
- [18] van Albada, T. S., Bahcall, J. N., Begeman, K., & Sancisi, R. (1985). Distribution of dark matter in the spiral galaxy NGC 3198. *Astrophysical Journal*, 295, 305–313. <https://doi.org/10.1086/163375>.
- [19] Walter, F., Brinks, E., de Blok, W. J. G., et al. (2008). THINGS: The HI Nearby Galaxy Survey. *The Astronomical Journal*, 136(6), 2563–2647. <https://doi.org/10.1088/0004-6256/136/6/2563>.
- [20] Wong, W. H., Wong, W. T., Wong, W. K., & Wong, L. M. (2014). Discovery of antigraviton verified by the rotation curve of NGC 6503. *International Journal of Advanced Astronomy*, 2(1), 1–7. <https://doi.org/10.14419/ijaa.v2i1.2244>.
- [21] Wong, W. T., & Wong, W. K. (2025). Quantum Gravity Theory Across Eight Galaxies: Precision Validation in NGC 925 and NGC 1569. *International Journal of Physical Research*, 13(2), 25–36. <https://doi.org/10.14419/z6vd0789>.
- [22] Zwicky, F. (1933). The Redshift of Extragalactic Nebulae. *Helvetica Physica Acta*, Vol. 6, p. 110-127, 1933.